

ROSAT OBSERVATIONS OF PULSED SOFT X-RAY EMISSION FROM PSR 1055–52

HAKKI ÖGELMAN^{1,2} AND JOHN P. FINLEY¹

Received 1993 April 29; accepted 1993 May 27

ABSTRACT

Utilizing the position-sensitive proportional counter and the high-resolution imager aboard the orbiting X-ray observatory *ROSAT*, we have detected pulsations at the radio period from the pulsar PSR 1055–52. The pulse shapes are energy-dependent and show a transition at ~ 0.5 keV where the phase angle of the pulse peak changes by $\sim -120^\circ$ and the pulsed fraction increases from 11% to 63% toward larger energies. Simple spectral models are found to be unsatisfactory, while multicomponent models, such as a soft blackbody and hard power-law tail, yield better fits to the pulse-height data. The hard power-law tail is consistent with the extension of the recently reported EGRET results and may indicate a common emission mechanism for the X-ray through GeV γ -ray regime. The soft blackbody component with $T_\infty = (7.5 \pm 0.6) \times 10^5$ K, if interpreted as the initial cooling of a neutron star, is consistent with standard cooling models and does not require the presence of exotic components.

Subject headings: pulsars: individual (PSR 1055–52) — stars: neutron — X-rays: stars

1. INTRODUCTION

PSR 1055–52 is a 197 ms pulsar with a period derivative of $5.8 \times 10^{-15} \text{ s s}^{-1}$ implying a dynamic age of $\tau = P/2\dot{P} \sim 5 \times 10^5 \text{ yr}$ and a rotational energy loss rate of $\dot{E} \sim 3 \times 10^{34} \text{ ergs s}^{-1}$. In an *Einstein Observatory* survey of radio pulsars carried out in the X-ray band PSR 1055–52 was one of the brightest sources detected (Cheng & Helfand 1983). The spectral results along with the absence of modulation at the pulsar spin period and evidence for angular extent led Cheng & Helfand (1983) to conclude that PSR 1055–52 is a compact object embedded in a mini-Crab nebula. Subsequent observations in the soft X-ray band were carried out in 1984 and 1986 with the *EXOSAT* satellite (Brinkmann & Ögelman 1987). The data required a soft X-ray spectrum characterized by a steep power law with a photon index $\alpha \leq -3.5$ or a blackbody spectrum with temperature in the range $(5\text{--}8) \times 10^5 \text{ K}$ (Brinkmann & Ögelman 1987). Poor statistics did not allow a meaningful limit to the modulation of the X-rays at the radio period, and the spatial resolution of the low-energy (LE) detector ($18''$) was insufficient to confirm the $10''$ extent as observed by the *Einstein* HRI. The soft spectrum and its consistency with a blackbody description led Brinkmann & Ögelman (1987) to conclude that the X-ray flux of PSR 1055–52 was a result of the initial cooling of a neutron star. PSR 1055–52 has recently been detected as a pulsed high-energy γ -ray source above 300 MeV with the EGRET telescope on board the *Compton Gamma Ray Observatory (CGRO)* (Fierro et al. 1993). In this *Letter* we present data acquired during 1990 and 1992 with the position-sensitive proportional counter (PSPC) and the high-resolution imager (HRI) aboard the X-ray satellite *ROSAT*. The observations are described in § 2. The temporal, spatial and spectral analyses are detailed in § 3, with a discussion of the results appearing in § 4.

2. OBSERVATIONS

PSR 1055–52 was observed with both the PSPC and the HRI at the focus of the X-ray telescope aboard *ROSAT* in the

¹ Department of Physics, University of Wisconsin–Madison, 1150 University Avenue, Madison, WI 53706.

² Max-Planck-Institut für Extraterrestrische Physik, D-8046, Garching, Germany.

energy range 0.1–2.4 keV. Detailed descriptions of the satellite, X-ray mirrors, and detectors can be found in Trümper (1983) and Pfeffermann et al. (1986).

The HRI observations were acquired during the calibration phase of the *ROSAT* mission from 1990 July 26 to 1990 July 28, with 8637 s effective exposure time. The PSPC observations were acquired during a 12 day span from 1992 January 4 to 1992 January 16; the total effective exposure time was 15,625 s.

The background-subtracted PSPC count rate of PSR 1055–52 in the 0.1–2.4 keV energy band, including vignetting and dead-time corrections, was $0.351 \pm 0.005 \text{ s}^{-1}$. The estimated background-subtracted HRI count rate was $0.066 \pm 0.003 \text{ s}^{-1}$.

3. RESULTS

3.1. Spatial

To investigate the existence of an extended component of PSR 1055–52, we utilized the data from the HRI. The $\sim 2''$ spatial resolution of the HRI can easily resolve an extended component with diameter $10''$ as reported by Cheng & Helfand (1983). To this end, we compared the radial count density profile of the source to the point-response function (PRF) of the HRI (see *ROSAT* Status Rep. 22 [1992]). After subtracting the linear combination of the HRI PRF and a flat background, a small residual remained. These residuals were then fitted adequately with a Gaussian with $\sigma = 3''.1 \pm 0''.3$ and 125 ± 40 total extra counts. The σ of this Gaussian is close to the $2''$ resolution of the HRI and probably reflects the convolution of attitude errors on a point-source profile. We consider this excess an upper limit and conclude that a diffuse component contributes $\lesssim 28\%$ of the 570 total counts observed from the source (2σ level) and is not consistent with the conclusions of Cheng & Helfand (1983).

3.2. Timing

The most unambiguous association of the X-ray source with PSR 1055–52 itself is the presence of X-ray pulsations at the radio period. To test for pulsations, the arrival times of the photons were reduced to the solar system barycenter using the JPL DE200 ephemeris and the J2000 coordinates of $\alpha = 10^{\text{h}}57^{\text{m}}58^{\text{s}}.76$, $\delta = -52^\circ 26' 56''.91$. Subsequently, we deter-

mined the arrival phases of the photons using the PSR 1055–52 radio ephemeris (Johnston et al. 1992). Throughout the observations, the frequency and the frequency derivative of the radio pulses were known to a sufficient accuracy that there was no need for any parameter search; in the case of the PSPC data each X-ray photon could also be directly phase-related to the radio pulse. The Z_1^2 statistic test (Buccheri et al. 1983) was then calculated for the PSPC and HRI data separately, yielding the values 19.6 and 16.6 with chance probabilities of 5.5×10^{-5} and 2.5×10^{-4} , respectively. Although the number of HRI photons was only 10% of the number of PSPC photons, the fact that the HRI signal was almost at the level of the PSPC signal indicated right away that the pulses had an energy-dependent shape and pulsed fraction. We further investigated this effect by examining the PSPC pulse shapes in different energy bands and discovered that the pulse shows a transition at ~ 0.5 keV both in the pulsed fraction and the phase of the peak. The top two panels of Figure 1 show this transition clearly, where we plot the phase and the pulsed fraction of the first harmonic as a function of the energy channel. Below channel 40 (~ 0.4 keV), the phase (the peak of the pulse) stays in the range 20° – 50° (with respect to the main peak of the radio pulse), and the pulsed fraction is around 0.1. Above channel 55, the phase angle jumps to values around 240° – 300° (or -60° to -120°), and the pulsed fraction increases from

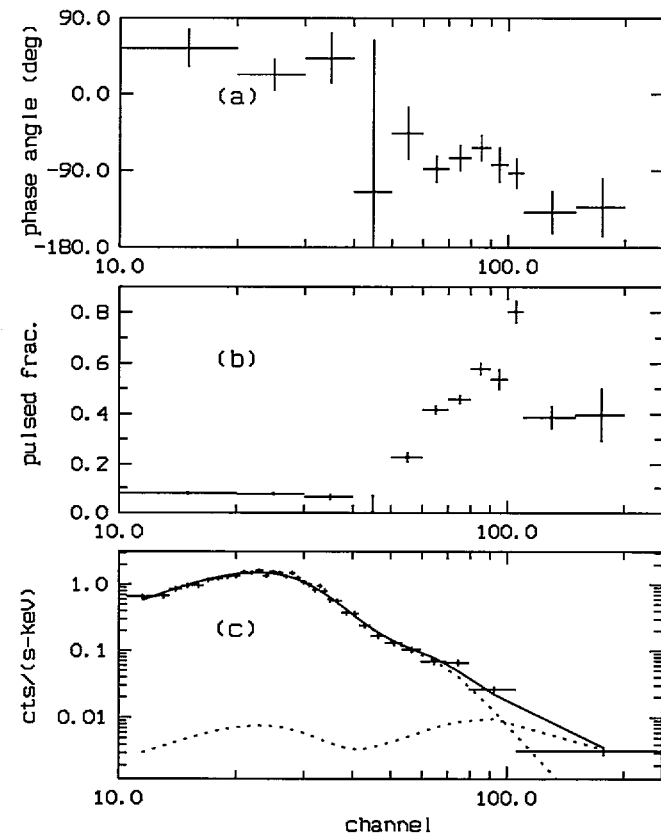


FIG. 1.—(a) Phase of the pulse peak, (b) pulsed fraction, and (c) observed pulse-height distribution, as a function of pulse-height channel. The two dashed curves in (c) are the fitted blackbody and *CGRO* power-law components whose sum is the solid line (see text). The energy in keV is approximately the channel number divided by 100. The phases and the pulsed fractions refer to the first harmonic only. The phase angle is with respect to the main peak of the radio pulse.

0.25 to a maximum of 0.85 around channel 100. If we consider the total below channel 45 and above channel 55, Z_1^2 is 31.7 for 5067 soft and 102.0 for 512 hard photons. Considering that Z_1^2 should be distributed as χ^2 with 2 degrees of freedom, the values above show clearly that the X-rays from PSR 1055–52 are pulsed at the radio period. For the first harmonic, the phase angles are $40^\circ \pm 2.5^\circ$ and $277^\circ \pm 1^\circ$, and the average pulsed fractions are $10.8\% \pm 0.3\%$ and $62.5\% \pm 0.5\%$ for soft and hard photons, respectively. These phase differences imply that the hard photons lead the soft by an angle of $123^\circ \pm 3^\circ$. Calculated from (mean – minimum)/mean, the soft and hard pulses have pulse fractions of 0.17 ± 0.06 and 0.73 ± 0.33 , respectively. This level of modulation is inconsistent with the 3% upper limit derived by Cheng & Helfand (1983). Figure 2 shows the soft and hard X-ray pulse profiles. In Table 1 we give the ephemeris used in determining the phases plotted in Figures 1 and 2. The epoch of zero phase has been calculated to correspond to the peak of the radio pulse. However, this absolute phasing should be considered as a preliminary result, since there is some concern that the calibration of the *ROSAT* spacecraft clock may contain an offset (Predehl, private communication).

3.3. Spectral

The dichotomy of the pulsed light curves above and below ~ 0.5 keV as discussed in § 3.2 already suggests that we must be dealing with a variety of processes. A blackbody model fitted to the pulse-height distribution of the PSPC photons further confirms this point. While a blackbody spectrum with a temperature in the range $(7-9) \times 10^5$ K fits the data well up to 0.7 keV, it leaves excess residuals at higher energies. We have also tried the modified blackbody models of Shibano et al. (1993) and Ventura et al. (1993), which include the effects of

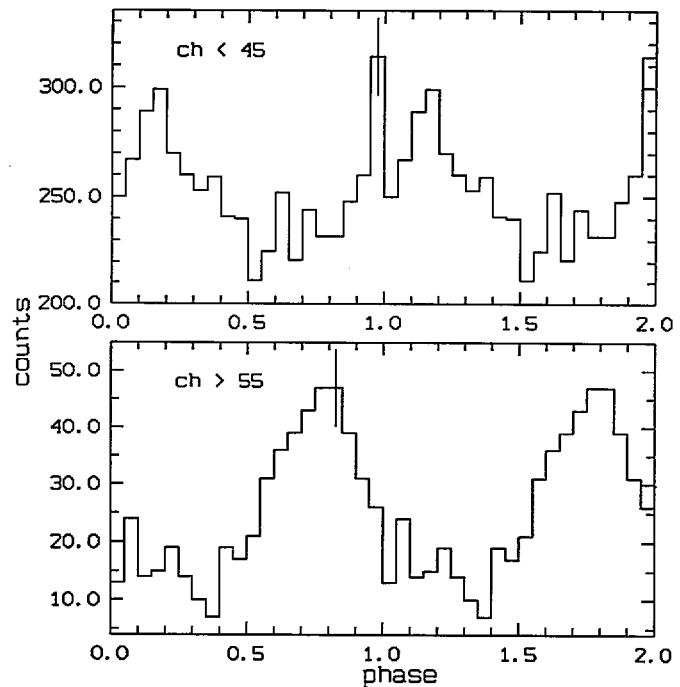


FIG. 2.—Folded light curves of PSR 1055–52 PSPC photons in the pulse-height channel range below 45 (top) and above 55 (bottom). The energy in keV is approximately the channel number divided by 100. Two cycles are shown for clarity. Phases 0 and 1 refer to the peak of the main radio pulse.

TABLE 1
SUMMARY OF RADIO PULSAR DATA USED IN PULSATION
ANALYSIS OF PSR 1055–52

| Date | Epoch ^a (TDB JD) | ν_0 (Hz) | $\dot{\nu}$ (Hz s ⁻¹) |
|----------------------------|--------------------------------|-----------------|--------------------------------------|
| 1992 Jan 4–16 (PSPC) | 2,448,629.652870169 | 5.073305083 | -1.50111×10^{-13} |
| 1990 Jul 26–28 (HRI) | 2,448,100.7453 | 5.073311945 | -1.5×10^{-13} |

^a The PSPC epoch is also the radio arrival time at the solar system barycenter in the barycenter dynamical time (TDB) scale. The HRI data were outside the range of the phase-related radio coverage of the *CGRO*/radio timing data base (Johnston et al. 1992).

atmospheric composition and the magnetic field. Although these models have a more extended high-energy tail, the fits were still not satisfactory. A power-law description ($dN/dE \propto E^{-\alpha}$) yields more acceptable results, but the spectral number index, $\alpha = 5.5$ – 6.0 , is very steep for typical power-law spectra, and the implied X-ray luminosity at the source is comparable to or exceeds the spin-down luminosity. Consequently, we performed two-component model fits in which we tried two-blackbody and blackbody-plus-power-law models. Table 2 summarizes these fits. The two-blackbody fits find a soft component with the larger flux and a temperature around $(7.0 \pm 0.6) \times 10^5$ K and a higher temperature component with $T \simeq (1.2$ – $3.5) \times 10^6$ K. The blackbody-plus-power-law fits basically find the same soft component blackbody parameters. For the power-law component, a large range of α and flux values give acceptable fits. These parameters are strongly correlated in the sense that steeper slopes have higher fluxes. We find in particular that if we restrict the power-law parameters to the $\pm 2\sigma$ range of the *CGRO*/EGRET results in the 100 MeV to 4 GeV range ($0.86 < \alpha < 1.50$), we find acceptable fits to the hard X-ray tail for $\alpha > 1.4$. Effectively, a single power law with this photon index can represent the high-energy spectrum of PSR 1055–52 in the keV to GeV range. We have included in Figure 1 the observed spectrum with the fitted values of this model.

4. DISCUSSION

With the detection of pulsed soft X-ray emission from PSR 1055–52, a group of four relatively old (10^4 to 5×10^5 yr)

pulsars appear to emerge as a family. In the order of increasing dynamical age, these are the Vela pulsar (Ögelman, Finley, & Zimmermann 1993), PSR 0656+14 (Finley, Ögelman, & Kızıloğlu 1992), Geminga (Halpern & Holt 1992; Halpern & Ruderman 1993), and PSR 1055–52. In X-rays, all four emit pulsed, soft, blackbody-like photons and have a high-energy tail. With the exception of PSR 0656+14, the members of the group emit γ -rays in the 100 MeV to GeV energy band with luminosities around 1%–50% of their rotational energy loss rates (Fierro et al. 1993). These pulsars, being the prime candidates for the detection of cooling neutron stars, suggest naturally a comparison with the existing theoretical cooling scenarios (Nomoto & Tsuruta 1987; Shibasaki & Lamb 1989; Page & Applegate 1992). The predictions of neutron star cooling theories are very sensitive to a number of parameters, such as exotic matter in the core, direct Urca processes (Lattimer et al. 1991), reheating, and superfluidity. Furthermore, the composition of the atmosphere and the surface magnetic field can substantially modify the emergent X-ray spectrum (Romani 1987; Miller 1992; Shibano et al. 1993; Ventura et al. 1993). Despite these complications, the softer blackbody temperature we fit for PSR 1055–52, $T_\infty = (7.5 \pm 0.6) \times 10^5$ K, matches perfectly the range of predictions of standard cooling curves with no exotic matter and no direct Urca mechanism (Nomoto & Tsuruta 1987; Page & Applegate 1992). The observed bolometric flux combined with the distance yields a radius of $R_\infty = (30 \pm 7) \times d(\text{kpc})$ km for the neutron star. The earlier estimate of the distance, based on the dispersion measure, was 920 pc (Manchester & Taylor 1981).

TABLE 2
SPECTRAL MODELS AND FIT PARAMETERS TO PSR 1055–52 IN THE ENERGY RANGE 0.1–2.4 keV

| Model | N_H (10^{20} cm ⁻²) | Model Parameter | f_x^a (keV cm ⁻² s ⁻¹) | χ^2/dof |
|---------------------------------------------------------------------|-----------------------------------------|--------------------------------------------------------------------------------------------------------|---------------------------------------------------------------------------------------------------------|---------------------|
| Single-Component Fits | | | | |
| Blackbody | 2.4 ± 0.8 | $kT = 70 \pm 5$ eV | $(4.8 \pm 1.2) \times 10^{-3}$ | 1.98 |
| Power-law ^b | 5.7 ± 1.0 | $\alpha = 5.8 \pm 0.5$ | $(1.9 \pm 0.9) \times 10^{-1}$ | 0.98 |
| Double-Component Fits | | | | |
| Blackbody (soft) plus Blackbody (hard) } | 3.5 ± 1.0 | $\left\{ \begin{array}{l} kT = 60 \pm 5 \text{ eV} \\ kT = 200 \pm 100 \text{ eV} \end{array} \right.$ | $\left\{ \begin{array}{l} (8 \pm 2) \times 10^{-3} \\ (1.2 \pm 0.7) \times 10^{-3} \end{array} \right.$ | 0.95 |
| Blackbody (soft) plus Power-law (hard) ^{b,c} } | 3.0 ± 1.0 | $\left\{ \begin{array}{l} kT = 60 \pm 5 \text{ eV} \\ \alpha = 1.4$ – $1.5 \end{array} \right.$ | $\left\{ \begin{array}{l} (7 \pm 2) \times 10^{-3} \\ (3 \pm 2) \times 10^{-5} \end{array} \right.$ | 1.15 |

NOTE.—Errors are 90% confidence limits.

^a f_x is the X-ray flux in the energy band 0.1–2.4 keV. For blackbody fits it is the bolometric flux.

^b The photon number flux $dN/dE \propto E^{-\alpha}$.

^c The hard power-law parameters of α and the flux have been restricted to the $\pm 2\sigma$ range ($0.86 < \alpha < 1.50$) measured at 100 MeV to 4 GeV with the *CGRO*/EGRET detector (Fierro et al. 1993).

With a more up-to-date Galactic electron density model the distance has been revised to 1.5 kpc (Taylor, Manchester, & Lyne 1993). Our results suggest that a distance of ~ 500 pc would give a more reasonable value of $R_\infty \sim 15$ km and also relieve the pressure of converting more than 30% of the spin-down luminosity to γ -rays (Fierro et al. 1993).

For Geminga, which appears to be a twin of PSR 1055–52 in many respects, Halpern & Ruderman (1993) have proposed a model in which a fraction of the e^\pm pairs accelerated in the outer gaps return to the polar caps and reheat them. Subsequently, the radiation from the heated polar caps encounters an optically thick cyclotron resonant atmosphere which reprocesses them to lower temperatures and spreads them over the whole surface of the neutron star, thus giving rise to the more intense lower temperature component. The harder X-ray photons are then explained as those that make it through the cyclotron backscattering region via the favorable polarization geometry. The γ -ray emission, which is an integral part of the model, comes from the curvature radiation of the outward-flowing e^\pm pairs. In principle, the same model can be applied to PSR 1055–52, as the two stars have very similar values of rotational energy loss, particle flow, and γ -ray luminosities. Despite these similarities, the total luminosity of the blackbody components of PSR 1055–52, $L_{\text{bol}} \sim (1.8 \pm 0.4) \times 10^{33} d^2 (\text{kpc}) \text{ ergs s}^{-1}$, is about an order of magnitude larger than the value predicted for Geminga by Halpern & Ruderman (1993) for maximal accelerator current. Possibly some fine-tuning of the model together with a distance of ~ 500 pc may reconcile the above model and the PSR 1055–52 observations.

The fact that we can fit the high-energy tail of the X-ray spectrum as the extension of the γ -ray power-law fit suggests

that a production mechanism of the single-power-law type may be generating photons in the range of X- to γ -rays. A further indicator of the common origin of these components is the fact that both the harder X-rays and the γ -rays have a high pulse fraction in the 50%–100% range. This interpretation of the observed X-ray spectrum requires no polar cap reheating and attributes the soft X-ray flux to thermal cooling radiation.

Another explanation of the phase shifts and the high-energy tail may involve the effects of the atmosphere and magnetic fields. In particular, the modified blackbody models of Shibano et al. (1993) and Ventura et al. (1993) do predict a crossover in the phase for perpendicular and parallel magnetic field geometries as well as a high-energy tail. Our attempts to fit the data to the case of a radial magnetic field geometry yield poor results (reduced χ^2 of 3.1) as well as predicted very low surface temperatures around 4.7×10^5 K. This would require the neutron star to be about 80 pc away if it had a sensible radius around 10 km. However, detailed modeling of a rotating hot neutron star with a dipole field may have more success.

The amount of detailed information that we have started to obtain from X-ray observations of nearby, middle-aged pulsars ($\sim 10^5$ yr) is becoming impressive. The results displayed in this *Letter* make it clear that we need more detailed models to explain the observations. Deeper exposures and a larger sample of sources may soon lead us to a consistent picture of pulsar magnetospheres and initial cooling.

We thank J. Fry, W. Kluźniak, W. Sanders, and J. Shaham for illuminating discussions, and G. Pavlov for providing us with tables of neutron star atmosphere models. This research was supported by NASA grant NAGW-2643.

REFERENCES

- Brinkmann, W., & Ögelman, H. 1987, *A&A*, 182, 71
 Buccheri, R., et al. 1983, *A&A*, 128, 245
 Cheng, A. F., & Helfand, D. J. 1983, *ApJ*, 271, 271
 Fierro, J. M., et al. 1993, *ApJ*, 413, L27
 Finley, J. P., Ögelman, H., & Kızılođlu, Ü. 1992, *ApJ*, 394, L21
 Halpern, J. P., & Holt, S. S. 1992, *Nature*, 357, 222
 Halpern, J. P., & Ruderman, M. 1993, *ApJ*, submitted
 Johnston, S., Kaspi, V., Manchester, R. N., & D'Amico, N. 1992, *GRO/Radio Timing Data Base*, Princeton University
 Lattimer, J. M., Pethick, C. J., Prakash, M., & Haensel, P. 1991, *Phys. Rev. Lett.*, 66, 2701
 Manchester, R. N., & Taylor, J. 1981, *AJ*, 86, 1954
 Miller, M. C. 1992, *MNRAS*, 255, 129
 Nomoto, K., & Tsuruta, S. 1987, *ApJ*, 312, 711
 Ögelman, H., Finley, J. P., & Zimmermann, H. U. 1993, *Nature*, 361, 136
 Page, D., & Applegate, J. H. 1992, *ApJ*, 394, L17
 Pfeiffermann, E., et al. 1986, *SPIE*, 733, 519
 Romani, R. W. 1987, *ApJ*, 313, 718
 Shibano, Yu. A., Zavlin, V. E., Pavlov, G. G., Ventura, J., & Potekhin, A. Yu. 1993, in *Isolated Pulsars*, ed. K. A. Van Riper, R. Epstein, & C. Ho (Cambridge: Cambridge Univ. Press), 174
 Shibasaki, N., & Lamb, F. K. 1989, *ApJ*, 346, 808
 Taylor, J., Manchester, R. N., & Lyne, A. G. 1993, preprint
 Trümper, J. 1983, *Adv. Space Res.*, 2, 241
 Ventura, J., Shibano, Yu. A., Zavlin, V. E., & Pavlov, G. G. 1993, in *Isolated Pulsars*, ed. K. A. Van Riper, R. Epstein, & C. Ho (Cambridge: Cambridge Univ. Press), 168